Technical Annals

Vol 1, No 6 (2024)

Technical Annals

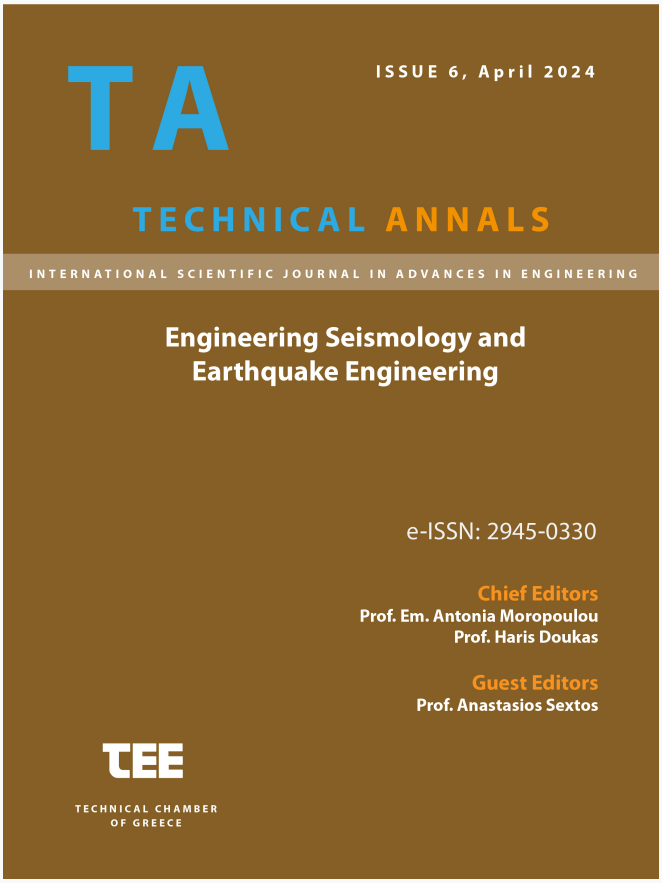

Experimental of the Tsonos model for predicting joint behavior in reinforced concrete frames

Emmanouil Golias

doi: 10.12681/ta.36757

To cite this article:

Golias, E. (2024). Experimental of the Tsonos model for predicting joint behavior in reinforced concrete frames. *Technical Annals*, *1*(6). https://doi.org/10.12681/ta.36757

Experimental of the Tsonos model for predicting joint behavior in reinforced concrete frames

Emmanouil A. Golias[1], Martha A. Karabini[1], Ioanna P. Vlasakidou[1], Filareti V. Papavasileiou[1], Emmanouil A. Vougioukas[2]

[1]Democritus University of Thrace, Kimmeria , Xanthi, Greece
[2]National Technical University of Athens 9, Iroon Polytechniou st., 15780 Athens, Greece
egkolias@civil.duth.gr

Abstract. Pushover analysis is widely regarded as the most accurate method for determining the bearing capacity of existing structures. To achieve a realistic assessment, it is essential to consider all possible failure modes. In many existing structures, joints are often designed with minimal or no transverse reinforcement, making joint failure more likely to occur before the failure of the connected members. This study employs a well-known joint behavior simulation to examine this scenario. The pushover analysis is terminated upon detecting joint failure, as it signifies a brittle failure. Analyses are performed on typical frames using both conventional criteria and the proposed joint failure criteria. The results are presented, ranked, and discussed.

Keywords: Beam-Column Joints, Design Criteria, Construction Joints.

1 Object of the research

Experience from earthquakes in Greece and worldwide has demonstrated that one of the most critical safety issues for reinforced concrete structures under seismic stresses is the occurrence of failures in the joint areas of column beams. These joints experience the highest shear forces and moments transferred from the ends of beams and columns. The joints' response to these highly cyclic actions should ideally remain elastic, avoiding any damage. However, if plastic deformation occurs, the joints must maintain their maximum strength during inelastic deformation cycles and absorb significant hysteretic energy.

Non-linear static (pushover) analysis is used to estimate the magnitude of inelastic deformations that structural elements will undergo during seismic events. This paper presents an experimental investigation that includes cyclic loading results for two full-scale 1:1 beam-column external joint specimens of medium ductility class, not in accordance with Eurocodes 2 and 8. The analytical part of the study examines the overall behavior of these experimental samples. Specifically, it evaluates an internationally recognized model from the literature for predicting the shear strength and failure modes of external joints.

The specimens are assessed using this model, particularly focusing on the collapse prevention framework established by Professor A.D. Tsonos. The paper aims to draw conclusions about the adequacy of construction joints and to determine whether well-constructed older buildings, which show no visible damage, remain fit for their intended purpose.

The geometry and the cross-section dimensions were common for all specimens for obvious comparison reasons; the total length of the column was 3.0 m and its cross section dimensions 350/250 mm whereas the length of the beam was 1.875 m and its cross section dimensions 350/250 mm. The reinforcing arrangements of all specimens are presented in **Fig. 1**. The compressive strength of the concrete used for the specimens was measured by supplementary compression tests of six standard D×h = 150×300 mm cylinders. The mean value at the age of 28 days was fc = 35,5 MPa. The steel of the longitudinal bars and the stirrups was S500 with yield tensile strength fy = 500 MPa.

Specimen 1

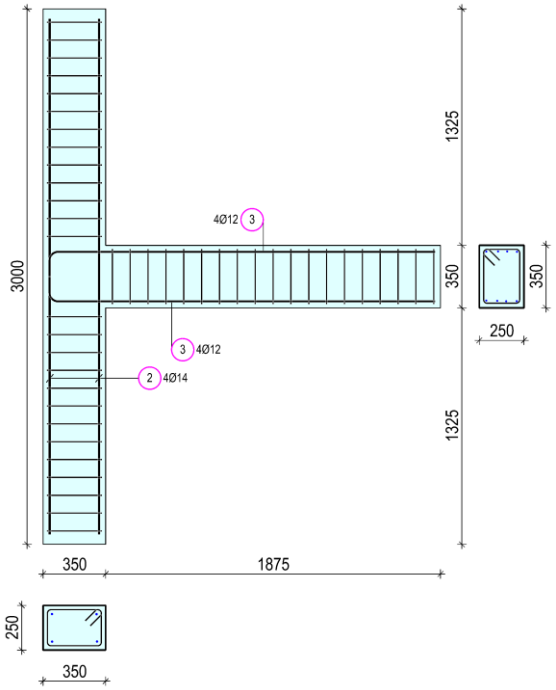

Specimen 2

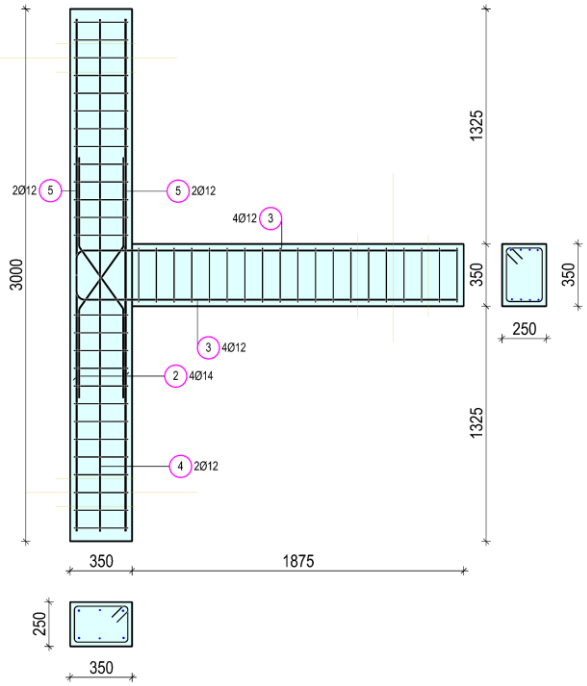

Fig. 1. Geometrical characteristics of the specimens 1 and Specimen 2

The beam in both Specimens 1 and 2 is reinforced with 4 bars of 12 mm diameter at the top and 4 bars of 12 mm diameter at the bottom (Fig. 1 and Table 1). The column reinforcement in Specimens 1 and 2 consists of 1Ø14 bars at the edges. In Specimen 2, there are also two pairs of X-type reinforcement bars 2Ø12 and two intermediate vertical bars Ø12. The stirrups in both the beam and column are the same in both specimens, Ø8/10. Detailed reinforcement is shown in Fig. 1.

The reinforcements of all specimens are presented in Fig. 1 and Table 1.

Table 1. Reinforcements in the joints of the specimens.

Reinforcements	Specimen 1	Specimen 2
①	-	-
②	2Ø14	2Ø14
③	4Ø12	4Ø12
④	-	2Ø12
⑤	-	2Ø12

2 Analytical models for behaviour predicting and failure modes

2.1 Cross Section Analysis

Next, an analysis of the cross-section of both the beam and the column is conducted to determine the actual flexural strength at the yielding of the tensile reinforcement.

Here's the interpretation of each symbol:

d: Effective depth of the section

ξ: Neutral axis coefficient

ε_c: Compressive strain in the concrete

f_y: Yield stress of the steel

f_{cm}: Compressive strength of concrete

x: Distance from the extreme compression fiber to the neutral axis d: Effective depth of the section

F_c: Compressive force in the concrete

ε_{s1}: Strain in the first steel reinforcement

ε_{sy}: Yield strain of the steel

ε_{s2}: Strain in the second steel reinforcement

E_s: Modulus of elasticity of the steel

σ_{s1}: Stress in the first steel reinforcement

σ_{s2}: Stress in the second steel reinforcement

ΣF: Sum of forces in the section

Specimen 1 and Specimen 2

BEAM 4Ø12 up[1]+down[2]							
$A_{s,prov} = 4.524$ cm² $d = 0.316$ m $d_1 = 0.034$ m $\varepsilon_c = -3.5$ ‰ $f_y = 500$ MPa f_{cm}=35.5 MPa	x_c (m)	$\lvert F_c \rvert$ (kN)	ε_{si} (‰)	σ_{si} (MPa)	F_{si} (kN)	$\sum F$	M_{Rb} (kN*m)
	0.033	236.54	1: 30.092	1: 500	1: 226.19	0	66.80
			2: 0.114	2: 22.88	2: 10.35		

Specimen 1

COLUMN 2Ø14 up[1]+down[2]							
$A_{s,prov} = 3.079$ cm² N=-122.5 kN $d = 0.315$ m $d_1 = 0.035$ m $\varepsilon_c = -3.5$ ‰ $f_y = 500$ MPa f_{cm}=35.5 MPa	x_c (m)	$\lvert F_c \rvert$ (kN)	ε_{si} (‰)	σ_{si} (MPa)	F_{si} (kN)	$\sum F - N$	M_{Rc} (kN*m)
	0.037	265.24	1: 26.363	1: 500	1: 153.94	0	61.00
			2: -0.182	2:-36.37	2:-11.20		

Specimen 2

COLUMN 2Ø14 left[1]+right[2] 2Ø12 in the middle[3]							
$A_{s,prov}$=3.079 cm² $A_{s,prov}$=2.262 cm² N=-122.5 kN $d = 0.315$ m $d_1 = 0.035$ m $\varepsilon_c = -3.5$ ‰ $f_y = 500$ MPa f_{cm}=35.5 MPa	x_c (m)	$\lvert F_c \rvert$ (kN)	ε_{si} (‰)	σ_{si} (MPa)	F_{si} (kN)	$\sum F - N$	M_{RC} (kN*m)
	0.048	335.53	1: 20.107	1: 500	1: 153.94	0	81.31
			2: 9.615	2: 500	2: 113.10		
			3: -0.877	3: -175.40	3: -54		

2.2 Theoretical Model

The model of the Professor of Antiseismic Structures of the Aristotle University of Thessaloniki, Alexandros Dimitrios Tsonos, focuses on the control and design of reinforced concrete beam-column joints. Using the model, the failure stress of the joint t_{ult} is calculated with great accuracy. When the applied shear stress in the joint is less than or equal to half the failure stress of the joint, $\tau_{cal} \leq 0.5\tau_{ult}$, then the joint in a strong earthquake will work in the elastic region safely driving the failure to the beam, where all the damage will concentrate leaving columns intact. In old buildings, the value of the proposed model is highlighted even more since it safely indicates which structural element (beam, column, joint) will cause failure initiation, and in general, it shows us the safe hierarchy of failures between these structural elements.

2.3 Capacity Check

Specimen 1

$\sum M_{RC} \geq 1.3 * \sum M_{Rb} \rightarrow 2 * M_{Rc} \geq 1.3 * M_{Rb} \rightarrow 2 * 61 \geq 1.3 * 66.80 \rightarrow 122 \geq 86.84$, which is satisfied

according to EN1998-1-§4.4.2.3.

Since, $\sum M_{RC} \geq \sum M_{Rb} \rightarrow 122\ \text{kN} * \text{m} > 66.80\ \text{kN} * \text{m}$, it will be valid for DCM:

- Finding Competent Design Shear Force of Beam

$$M_{1d} = \gamma_{Rd} * M_{Rb} = 1 * 66.80 = 66.80\ \text{kN} * \text{m},$$
$$V_{capacity} = \frac{M_{1d}}{l_{cl}} = \frac{66.80}{1.475} = 45.29\ \text{kN}$$

- Finding Competent Design Shear Force of Column

$$M_{1d} = M_{2d} = \gamma_{Rd} * M_{Rc} = 1.1 * 2 * 61 = 134.20\ \text{kN} * \text{m}$$
$$V_{capacity} = \frac{M_{1d}}{l_{cl}} = \frac{134.20}{2.50} = 53.68\ \text{kN}$$

Specimen 2

$\sum M_{RC} \geq 1.3 * \sum M_{Rb} \rightarrow 2 * M_{Rc} \geq 1.3 * M_{Rb} \rightarrow 2 * 81.31 \geq 1.3 * 66.80 \rightarrow 162.62 \geq 86.84$, which is satisfied according to EN1998-1-§4.4.2.3.

Since, $\sum M_{RC} \geq \sum M_{Rb} \rightarrow 162.62\ \text{kN} * \text{m} > 66.80\ \text{kN} * \text{m}$, it will be valid for DCM:

- Finding Competent Design Shear Force of Beam

$$M_{1d} = \gamma_{Rd} * M_{Rb} = 1 * 66.80 = 66.80\ \text{kN} * \text{m},$$

$$V_{capacity} = \frac{M_{1d}}{l_{cl}} = \frac{66.80}{1.475} = 45.29\ \text{kN}$$

- Finding Competent Design Shear Force of Column

$$M_{1d} = M_{2d} = \gamma_{Rd} * M_{Rc} = 1.1 * 2 * 81.31 = 178.882\ \text{kN} * \text{m}$$

$$V_{capacity} = \frac{M_{1d}}{l_{cl}} = \frac{178.882}{2.50} = 71.56\ \text{kN}$$

2.4 Application of Tsonos Model (2007-2019)

Specimen 1

Initially, the increased compressive strength of the concrete due to overtightening is calculated, using the model of Scott at al. (1982)

$$h_o = h_c - 2 * c_{nom} - 2 * \emptyset_w/2 = 350 - 2 * 20 - 2 * 4 = 302\ \text{mm}$$

$$b_o = b_c - 2 * c_{nom} - 2 * \emptyset_w/2 = 250 - 2 * 20 - 2 * 4 = 202\ \text{mm}$$

$$\rho_s = 0, \qquad k = 1 + \frac{\rho_s * f_{yw}}{f_c'} = 1, \qquad f_c = k * f_c' = 1 * 35.5 = 35.5\ \text{MPa}$$

$$\alpha = \frac{h_b}{h_c} = \frac{350}{350} = 1.0$$

The system of equations (1), (2) and (3) is solved:

$$x = \frac{\alpha \cdot \gamma_{ult}}{2\sqrt{f_c}} \quad (1), \quad \psi = \frac{\alpha \cdot \gamma_{ult}}{2\sqrt{f_c}} \cdot \sqrt{1 + \frac{4}{a^2}} \quad (2), \quad x - \psi = -0.1 \quad (3)$$

resulting in:

- The failure deformation of the joint: $\gamma_{ult} = 0.96$
- The failure stress of the joint:

$$\tau_{ult} = \gamma_{ult} * \sqrt{f_c} = 0.96 * \sqrt{35.5} = 5.72\ \text{MPa}$$

- Horizontal shear force at the external joint, when a flexural crack forms in the beam:

$$V_{cal} = 1.25 * A_{s1} * f_y - V_{col} = 1.25 * 4.52 * 500 * 10^{-1} - 29.89 = \ 252.61 \text{ kN}$$

Based on the geometry of the specimen, it follows that, when the maximum shear force develops in the beam, then a shear force develops in the column is equal to:

$$V_{col} = V_{Ed,max} * \frac{l}{h} = 45.29 * \frac{1.475 + \left(\frac{0.35}{2}\right)}{2.5} = 29.89 \text{ kN}$$

- The deformation in the joint, when the beam fails:

$$\gamma_{cal} = \frac{V_{cal}}{h_c * b_c * \sqrt{f_c}} = \frac{252.61 * 10^3}{0.35 * 0.25 * \sqrt{35.5} * 10^6} = \ 0.485$$

- The shear stress exerted on the joint, when the beam fails:

$$\tau_{cal} = \gamma_{cal} * \sqrt{f_c} = 0.485 * \sqrt{35.5} = 2.89 \text{ MPa}$$

Since, $\tau_{cal} < \tau_{ult}$, the yielding of the beam will be preceded.

SPECIMEN 2

$$\rho_s = A_{sw} * \frac{2b_o \ + \ 2h_o}{b_o * \ h_o \ * \ s} = 4.524 * \frac{2 * 20.2 \ + \ 2 * 30.2}{20.2 * \ 30.2 \ * \ 35} = 0.0214$$

$$k = 1 + \frac{\rho_s * f_{yw}}{f_c'} = 1 + \frac{0.0214 * 500}{35.5} = 1.3 \, , \qquad f_c = k * f_c' = 46.2 \text{ MPa},$$

$$\alpha = \frac{h_b}{h_c} = 1.0$$

The system of equations (1), (2) and (3) is solved. Resulting in:

- The failure deformation of the joint: $\gamma_{ult} = 1.1$
- The failure stress of the joint:

$$\tau_{ult} = \gamma_{ult} * \sqrt{f_c} = 1.1 * \sqrt{46.2} = 7.48 \text{ MPa}$$

- Horizontal shear force at the external joint, when a flexural crack forms in the beam:

$$V_{cal} = 1.25 * A_{s1} * f_y - V_{col} = 1.25 * 4.52 * 500 * 10^{-1} - 47.23 = \ 235.27 \text{ kN}$$

Where,

$$V_{col} = V_{capacity} * \frac{l}{h} = 71.56 * \frac{1.475 + \left(\frac{0.35}{2}\right)}{2.5} = 47.23 \text{ kN}$$

- The deformation in the joint, where the beam fails:

$$\gamma_{cal} = \frac{V_{cal}}{h_c * b_c * \sqrt{f_c}} = \frac{235.27 * 10^3}{0.35 * 0.25 * \sqrt{46.2} * 10^6} = \ 0.4$$

- The shear stress exerted on the joint, when the beam fails:

$$\tau_{cal} = \gamma_{cal} * \sqrt{f_c} = 0.4 * \sqrt{46.2} = 2.7 \text{ MPa}$$

Since $\tau_{cal} < \tau_{ult}$, the yielding of the beam will be preceded.

3 Experimental program

3.1 Experimental Layout

Test rig and setup along with the instrumentation details are shown in Fig. 2. Each beam-column specimen is rotated 90º, so that the beam is in the vertical direction and the column in the horizontal direction. Supporting devices that allow rotation are used to simulate the inflection points in the middle of the column height in a real laterally loaded frame.

Column compressive axial load N_c equal to $N_c=0.05A_cf_c$ was constantly applied during the experimental procedure in all specimens. The value of the column axial load was controlled to remain constant during the loading procedure at the level of N_c=150 kN for all specimens. Although the influence of a variation of axial load values is not examined in this study, the effect of high axial load on the shear capacity of beam–column joints can be considered as favourable. On the other hand, varying the axial load during the test can lead to low level of axial load in some steps of the test, which would tend to emphasize a weak column–strong beam hierarchy. This could lead to a possibility of a predominant flexural behaviour due to column hinging.

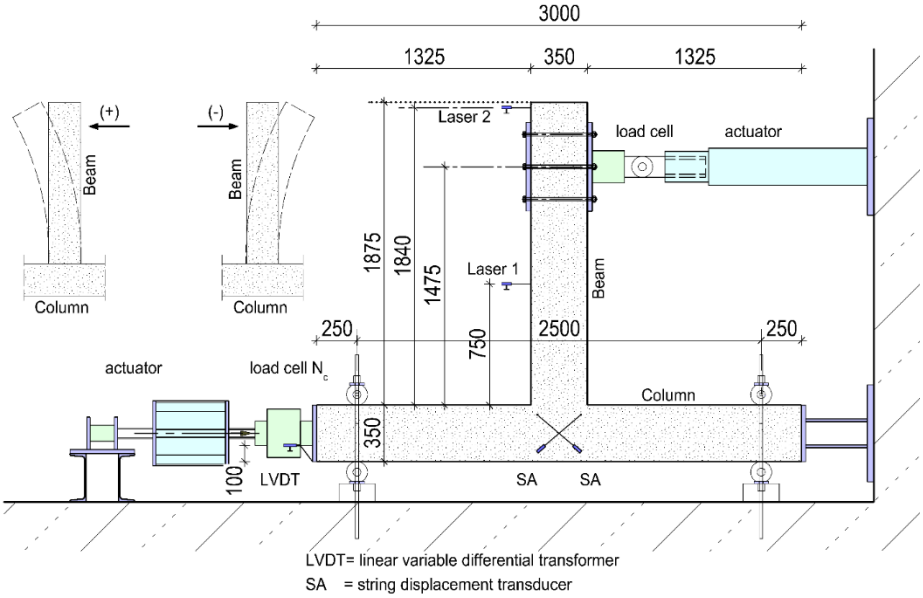

Fig. 2. Experimental layout

3.2 Load History

All specimens were subjected to the same loading sequence. They were subjected to full cyclic deformation imposed near the free and of the beam which as it can be observed in the test setup is in the vertical direction (Fig. 2). The moment arm for the applied load is equal to 1.475m.

Tested specimens suffered seven loading steps with maximum displacements equal to ±8.5mm, ±12.75mm, ±17.0mm, ±25.5mm, ±34.0mm, ±51.0mm and ±68.0mm at each step, respectively. Each of the seven loading steps included three full loading cycles; thus the loading sequence was performed the way it is shown in Fig. 3. All beam-column joints were subjected to full-cycle deformations. The specimens were subjected to an eight-step loading history. Each loading step consists of three full loading cycles.

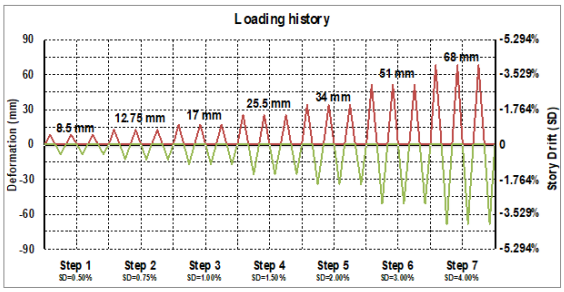

STEP	SD	δ
	(%)	(mm)
1	0.50	8.50
2	0.75	12.75
3	1.00	17.00
4	1.50	25.50
5	2.00	34.00
6	3.00	51.00
7	4.00	68.00
8	5.00	85.00

Fig. 3. Loading sequence. Eight loading steps and each step includes three full loading cycles

To effectively use results from quasi-static cyclic loading tests on reinforced concrete structural elements for overall performance evaluation, it is crucial to establish a loading history that encompasses both the critical capacity issues of the element and the seismic demands. In inelastic seismic scenarios, capacity and demands are interdependent, with each potentially influencing the other. Key seismic capacity parameters for a structural element include strength, stiffness, inelastic deformation capacity (ductility), and cumulative damage capacity, such as energy dissipation. These parameters are expected to deteriorate with an increase in the number of damaging cycles and the amplitude of the cycles.

Every inelastic excursion results in cumulative damage to a structural element. The adopted loading program emphasizes a multi-cycle loading sequence, as repeated loading cycles can cause damage similar to that seen after moderate seismic events, which is a focus of this investigation. Therefore, each loading step in the program includes three full loading cycles, and the entire program consists of steps with progressively increasing displacements (Fig. 3). The effects of loading sequence have not been thoroughly researched, and the sequence of large versus small excursions in a structural element during a severe earthquake does not follow a consistent pattern. The number of inelastic excursions increases as the period of the structural system decreases, with a particularly high rate of increase for short-period systems.

It is important to recognize that seismic demands on structures depend on numerous variables, and a single loading history will always involve some compromise. However, a conservative loading program for most practical cases must be applied. Thus, the chosen loading program is a comprehensive cumulative damage testing approach that allows the determination of structural

performance parameters. These parameters, combined with a cumulative damage model, can be used to evaluate performance under various seismic excitations.

3.3 Hysteretic Response Diagrams

To understand some important details regarding the acquired experimental hysteretic response of the tested samples, Fig. 4a and 5a present the load versus slip curves for each loading step. Each step includes three loading cycles. The points where cracking initiated are marked on the diagrams for the first cycles of step 1 for both loading directions (positive and negative).

Furthermore, steel yielding due to the propagation of damage caused by the increased applied load may also lead to more extensive damage during the initial cycles of steps 5, 6, and 7.

As the imposed displacement on Specimens 1 and 2 increased (steps 5 and 6), it led to an increase in the crack width at the beam's initial section (damage concentration), while at step 7, cracks were also observed at the joint area. Although damage was concentrated in the beam area, cracks also appeared in the joint body.

In Specimen 2, a better performance is observed in the joint area due to the contribution of the X-type reinforcements. The plastic hinge is formed clearly in the beam, which is the desired outcome. Minimal cracking is observed in the joint area.

The load-bearing capacity for both specimens remains approximately at the same level. Fig. 4b and 5b.

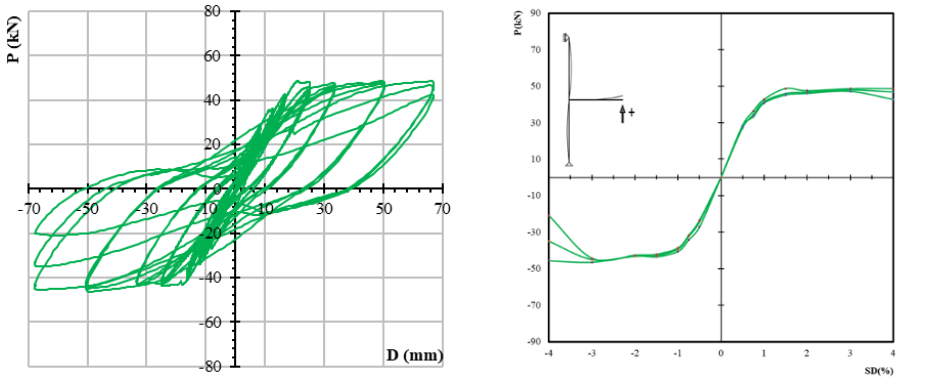

(a) Hysteretic Response (b) Envelope curves of maximum loads at all cycles

Fig. 4. Hysteretic response and load envelope of all cycles of Specimen 1

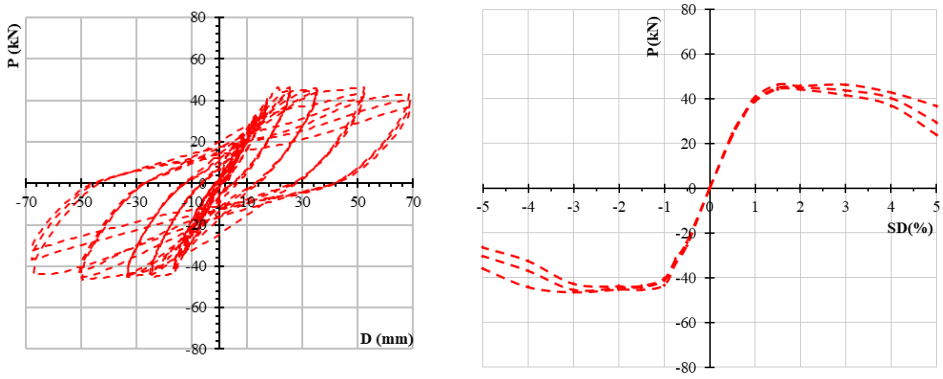

(a) Hysteretic Response (b) Envelope curves of maximum loads at all cycles

Fig. 5. Hysteretic response and load envelope of all cycles of Specimen 2

4 Conclusions

In this work, the application of the Tsonos model to two specimens was rigorously analyzed and compared with the corresponding experimental results. The study aimed to evaluate the model's effectiveness in predicting the behavior of reinforced concrete beam-column joints, particularly under seismic loading conditions. The Tsonos model focuses on calculating key parameters such as joint failure stress and the stress at beam failure, which are critical for assessing the structural integrity and safety of such joints.

The results of the analysis demonstrated that the Tsonos model could accurately predict the joint failure stress and the stress at beam failure. The model's predictions closely matched the observed experimental data, with only minor deviations. This high level of accuracy indicates that the model can effectively capture the complex interactions and stress distributions that occur within the joint during loading.

A key finding from the study was that the yielding of the beam occurred prior to any significant failure at the joint. This observation is crucial because it suggests that the Tsonos model accurately predicts the sequence of failure events, which is essential for designing safe and reliable structures. Ensuring that beams yield before joints fail is a fundamental principle in structural design, as it allows for energy dissipation and prevents catastrophic collapse.

The study concluded that both the analytical calculations based on the Tsonos model and the experimental results were in excellent agreement. This alignment validates the Tsonos model as a reliable tool for predicting the performance of beam-column joints in reinforced concrete structures. The model's accuracy and reliability make it a valuable asset for engineers seeking to design buildings that can withstand seismic forces without experiencing critical structural failures.

However, it is important to note that the conclusions drawn from this study are primarily qualitative. While the qualitative observations support the model's reliability, future work should focus on providing quantitative comparisons. This involves detailed explanations and discussions that relate the experimental results to the assumptions and

conditions of the analytical model, such as the specifics of the experimental setup and loading conditions. Providing such detailed quantitative analysis would further solidify the confidence in the Tsonos model and clarify its limitations and applicability in various structural scenarios.n this work, the application of the Tsonos model to the two samples was examined and a comparison was made with the experimental results. In particular, applying Tsonos' theoretical model, the joint failure stress and the joint stress at beam failure are calculated with excellent accuracy. Based on these, it follows that the yielding of the beam will precede the joint. It is concluded that both calculations and experimental tests are in complete agreement. It thus proves that the "Tsonos model" is a reliable model for designing joints and preventing the collapse of reinforced concrete buildings.

Specimen 1

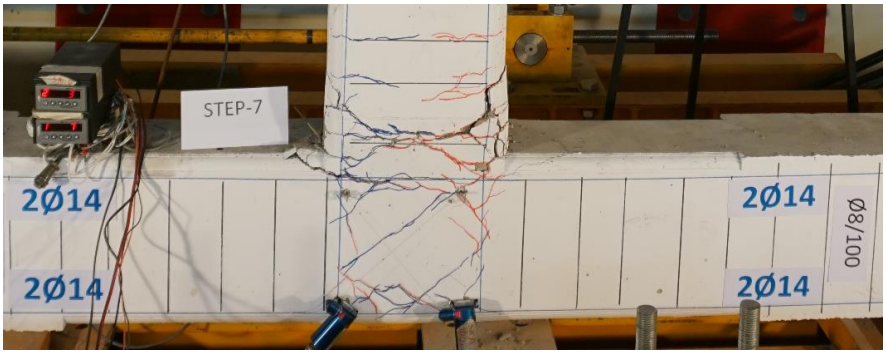

Specimen 2

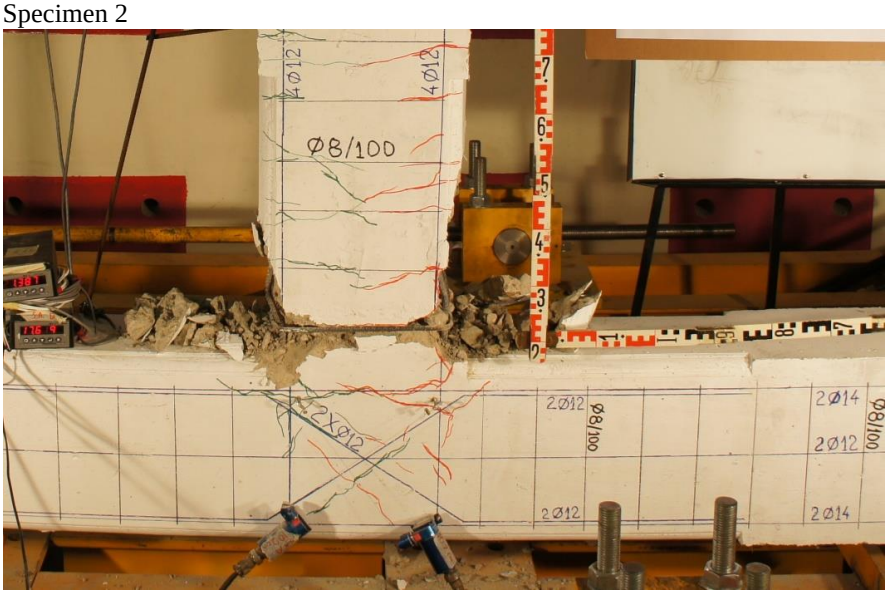

Fig. 6. Final state of damage to the beams of specimens

References

1. Karagiannis, C.G. "Design of Reinforced Concrete Structures' Behavior Against Earthquakes." Sofia A.E. Publishing, Thessaloniki, 2013, pp. 320, 463, 475.
2. Scott, A., Park, R., & Priestley, M. J. N. (1982). "Seismic resistance of reinforced concrete beam-column joints." *Journal of Structural Engineering*, 108(4), 891-912
3. Tsonos A.G. (2010), "Performance enhancement of R/C building columns and beam-column joints through shotcrete jacketing", Engineering Structures, 32, 726-740.
4. Tsonos, A.D. "Towards a New Approach in the Design of Beam-Column Joints in Reinforced Concrete." *Technical Chronicles, Scientific Edition of TEE, Scientific Section A,* Jan.–Aug. 1996, Vol. 16, No. 1-2, pp. 69-82.
5. Tsonos A.G. (2007), "Cyclic load behavior of reinforced concrete beam-column subassemblages of modern structures", ACI Structural Journal, 194(4), 468-478.
6. Tsonos, A.D. "Design of Reinforced Concrete Structures According to Eurocodes." Sofia A.E. Publishing, Thessaloniki, 2017, pp. 231, 232, 240-242.
7. Karayannis C.G. & Golias E. "Strengthening of deficient RC joints with diagonally placed external C-FRP ropes" Journal Earthquakes and Structures, Vol. 20 No. 1 (2021), 123-132.
8. DOI: https://doi.org/10.12989/eas.2021.20.1.123
9. Karayannis, C.G., Golias, E. "Full-scale Experimental Testing of RC Beam-column Joints Strengthened using CFRP Ropes as External Reinforcement."
10. Engineering Structures 2022, 250,113305.
11. https://doi.org/10.1016/j.engstruct.2021.113305
12. Pohoryles, D.A., J. Melo, T. Rossetto, H. Varum. 2019. "Seismic Retrofit Schemes with FRP for Deficient RC Beam-Column Joints: State-of-the-Art Review." J. Compos. Constr., 23(4): 03119001.
13. https://doi.org/10.1061/(ASCE)CC.1943-5614.0000950.
14. Al-Mahmoud F., Castel, A., François, R., C. Tourneur. 2009. "Strengthening of RC members with near-surface mounted CFRP rods", Composite Structures, 91(2), pp. 138-147.
15. Yurdakul Ö, Ö. Avşar. 2016. "Strengthening of substandard reinforced concrete beam-column joints by external post-tension rods." Engineering Structures, 107, 9-22.